Study of adaptive control algorithm using hysteretic magneto-rheological damper model in 1/4 car suspension

JURAJ ÚRADNÍČEK*, MILOŠ MUSIL

This paper presents a study of the semiactive adaptive control algorithm through numerical simulation where the adaptive control is compared to the widely used skyhook control and passive suspension. A hysteretic magneto--rheological (MR) damper model is developed so that sensitivity of the system variables with respect to the control variable can be evaluated for the purpose of employing the adaptive control algorithm based on the gradient search method. This study includes discussions of the MR damper model setup, a 1/4 car suspension model setup, dynamic analysis approach and tuning of the controllers parameters as well as passive damping. The dynamic analysis is performed in the time domain using sine sweep excitation without the need to linearize such a nonlinear semiactive system. Through simulations, the effectiveness of both controllers and passive suspension is demonstrated for vibration isolation. Effectiveness of all setups under high frequency random excitation for why the suspension is not optimally tuned is demonstrated to study adaptability of the setups under different driving conditions.

K e y w o r d s: adaptive control, skyhook control, hysteretic MR damper model, 1/4 car suspension, controller tuning, dynamic simulation

1. Introduction

Since Semiactive control policy was first developed by Karnopp and Crosby in 1973, great attention has been paid to the development of a semiactive suspension for automotive applications, which introduced many improvements of the original Skyhook strategy proposed in [1].

Non-model based Skyhook control is a bi-state control policy, which is along its variations widely used in a seats suspension or car suspension assembly. The amount of dissipated energy in a semiactive damper is controlled through the changing of damper characteristics. Even though the skyhook is a relatively simple and low-cost policy verified by many years of usage, there are some circumstances when skyhook could yield adverse results. One of the main disadvantages of the skyhook

SjF STU, Nám. slobody 17, 812 31 Bratislava, Slovak Republic
* Corresponding author, e-mail address: juraj.uradnicek@stuba.sk

policy is the result of higher harmonics occurring in a system, which should nevertheless have pure tone signals accessing it. This higher harmonic is the cause of nonlinearity due to switching between two states of controlled semiactive damper. Another disadvantage is the dynamic jerking occurring due to phase delay as a result of the application of filters to derive relative velocity from the measured displacement signal. These dynamic phenomena are explained in [2]. The third non-negligible weakness of the skyhook is its poor adaptability to plant variations or different excitation profiles. Skyhook gain is pre-tuned in certain conditions according to a performance index. Changing these conditions can lead to worse or even adverse performance.

Mentioned disadvantages of the skyhook strategy can be attenuated introducing an adaptive control strategy, which can control damper characteristics continuously [3]. Since the performance index is evaluated in real time, such a strategy can react to the plant and road variations immediately. Other different control strategies of the semiactive suspension systems are discussed in [14, 15].

Reasonable MR damper model should be employed in order to use the model-based adaptive control algorithm, which requires the calculation of the sensitivity of controlled variables with respect to the control current applied to the MR damper. Modelling of MR damper is discussed in [4–6, 13]. Experimental study of MR dampers is closely discussed in [7]. The main advantage of model proposed in this work is its continuous mathematical description which is necessary in sense of adaptive algorithm utilization discussed further.

2. Modelling of semiactive MR damper

In order to use the model-based adaptive control algorithm a simple hysteretic semiactive MR damper model has been proposed to ensure easy differentiability of a whole system model with respect to the control current I. Force F_{MR} produced in the MR damper is calculated from

$$F = c\dot{y}_{\mathrm{r}} + ky_{\mathrm{r}} + \alpha z + F_0, \tag{1a}$$

$$z = \tanh(\beta\, \dot{y}_{\mathrm{r}}), \tag{1b}$$

$$\dot{s} = -fs + h_3 F, \tag{1c}$$

$$F_{\mathrm{MR}} = f\, s + h_2 F. \tag{1d}$$

Mentioned mathematical model can be presented schematically as shown in the Fig. 1.

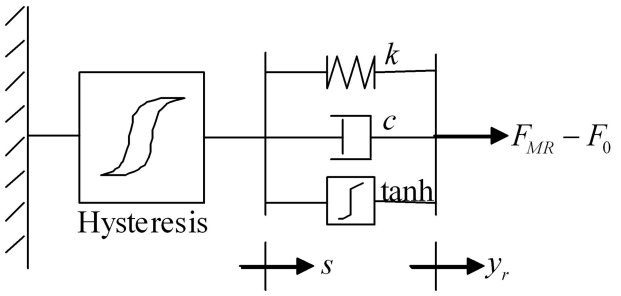

Fig. 1. Schematic of the MR damper model.

Variables c, k, α, F_0 depend on the control current I in the following way [8]:

$$c = c_1 I + c_0, \tag{2a}$$

$$k = k_1 I + k_0, \tag{2b}$$

$$\alpha = \alpha_2 I^2 + \alpha_1 I + \alpha_0, \tag{2c}$$

$$F_0 = h_1 I + h_0. \tag{2d}$$

Substitution of Eqs. (2a)–(2d) into Eq. (1a) leads to

$$\begin{aligned} F &= (c_1 \dot{y}_\mathrm{r} + k_1 y_\mathrm{r} + h_1 + \alpha_1 z) I + (c_0 \dot{y}_\mathrm{r} + k_0 y \in + h_0 + \alpha_0 z + \alpha_2 I^2 z) \\ &= B_1 I + D_1, \end{aligned} \tag{3}$$

where $B_1 = c_1 \dot{y}_\mathrm{r} + k_1 y_\mathrm{r} + h_1 + \alpha_1 z$ and $D_1 = c_0 \dot{y}_r + k_0 y_r + h_0 + \alpha_0 z + \alpha_2 I^2 z$ are non-linear functions which describe MR damper characteristics. In contrast to the model proposed in [8], typical hysteretic behaviour of MR damper is provided as a phase lag of MR damper force to piston velocity $\dot{y}_\mathrm{r}$ by the first order filter described in (1c). Variable s is a state variable of the filter. Parameter f in (1c), (1d), which can be either constant or a function of current I, is describing the size of calculated hysteretic loop in the model characteristics. Finally MR damper force F_MR is calculated from (1d). Computed MR damper characteristics using the proposed model are shown in Fig. 2.

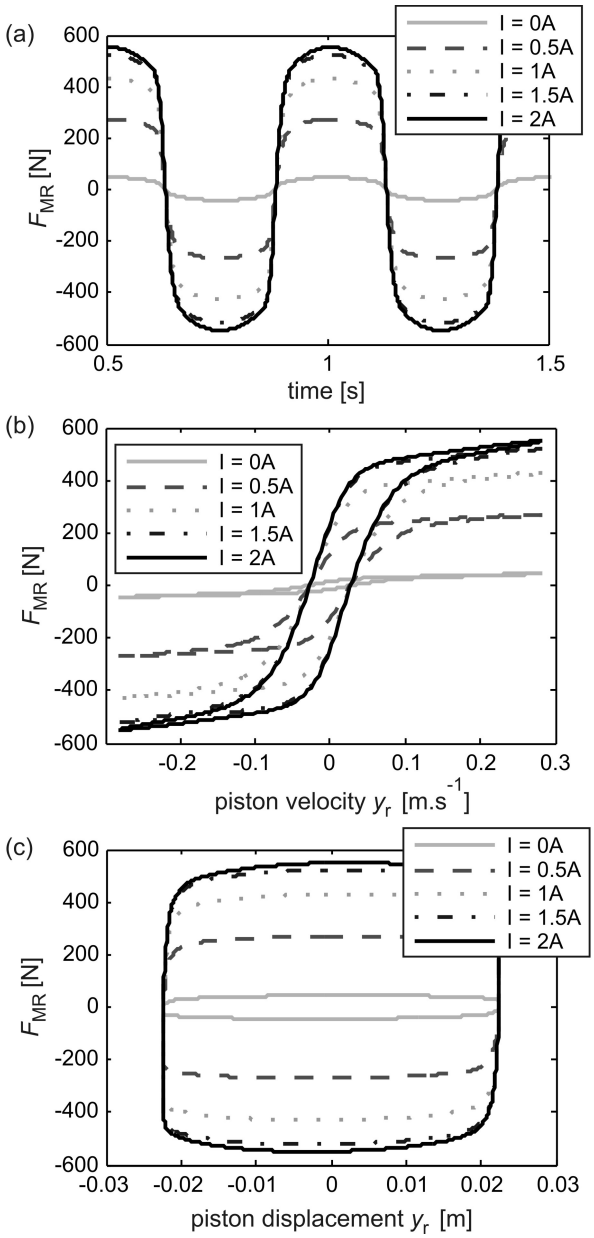

Fig. 2. Computed characteristic of the MR damper model: a) damping force vs. time, b) damping force vs. piston velocity, c) damping force vs. piston displacement.

3. Control strategy

Two different control strategies are considered to control the tunable current I to the MR damper. First approach is based on a no-jerk skyhook control policy, which is represented as

$$I = \begin{cases} 0, & \dot{y}_1 y_r \leq 0 \\ S\dot{y}_1 y_{\mathrm{r}}, & \dot{y}_1 y_{\mathrm{r}} > 0 \end{cases}, \tag{4}$$

where S is the skyhook gain, $\dot{y}_1$ is velocity of sprung mass (Fig. 3), $\dot{y}_r = \dot{y}_1 - \dot{y}_2$ is MR damper piston velocity.

Second control approach has been specially designed for nonlinear vibration systems with unknown random vibration excitation [9]. Model-based nonlinear control algorithm always tries to minimize the performance index (5) regardless of plant variations and on-going unknown excitations:

$$J = J(\dot{\boldsymbol{x}}, \boldsymbol{x}), \tag{5}$$

$\boldsymbol{x}$ is a vector of state variables of a system represented by dynamic equations

$$\dot{\boldsymbol{x}} = f(\boldsymbol{x}, F_{\mathrm{MR}}). \tag{6}$$

Control current I is tuned by the following adaptive control law:

$$I(t + \Delta T) = I(t) + \mu \left(-\frac{\partial J(t)}{\partial I(t)} \right). \tag{7}$$

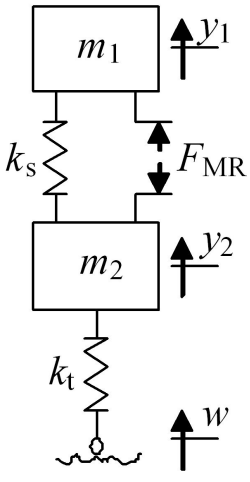

Fig. 3. Scheme of the simulated dynamical system.

Performance index sensitivity with respect to the control current $\partial J/\partial I$ can be found by solving the equation

$$\frac{\partial J}{\partial I} = \frac{\partial J}{\partial \dot{\boldsymbol{x}}}\frac{\partial \dot{\boldsymbol{x}}}{\partial I} + \frac{\partial J}{\partial \boldsymbol{x}}\frac{\partial \boldsymbol{x}}{\partial I}, \tag{8}$$

expressions $\partial J/\partial \dot{\boldsymbol{x}}$ and $\partial J/\partial \boldsymbol{x}$ can be obtained by differentiating (5), moreover, state variable sensitivity $\partial \dot{\boldsymbol{x}}/\partial I$, $\partial \boldsymbol{x}/\partial I$ can be obtained from dynamic equations (6) after differentiating with respect to the control current I:

$$\frac{\partial \dot{\boldsymbol{x}}}{\partial I} = \frac{\partial f(\boldsymbol{x}, F_{\mathrm{MR}})}{\partial I}. \tag{9}$$

4. Suspension system description

The following quarter car model (Fig. 3) has been modelled for the purpose of numerical simulation:

The damping force FMR shown in the Fig. 3 is the force generated in the MR damper. Dynamics of this lumped mass system is represented by the dynamic equations

$$\begin{bmatrix} m_1 & 0 \\ 0 & m_2 \end{bmatrix}\begin{bmatrix} \ddot{y}_1 \\ \ddot{y}_2 \end{bmatrix} + \begin{bmatrix} k_{\mathrm{s}} & -k_{\mathrm{s}} \\ -k_{\mathrm{s}} & k_s + k_{\mathrm{t}} \end{bmatrix}\begin{bmatrix} y_1 \\ y_2 \end{bmatrix} + \begin{bmatrix} 1 \\ -1 \end{bmatrix} F_{\mathrm{MR}} = \begin{bmatrix} 0 \\ k_{\mathrm{t}} \end{bmatrix} w. \tag{10}$$

Equations (10) can be rewritten as

$$\mathbf{M}\ddot{\boldsymbol{y}} + \mathbf{K}\boldsymbol{y} + \boldsymbol{p}F_{\mathrm{MR}} = \boldsymbol{m}w, \tag{11}$$

the state variables sensitivity with respect to the control current can be obtained differentiating dynamic equations (11) with respect to the control current as follows:

$$\mathbf{M}\frac{\partial \ddot{\boldsymbol{y}}}{\partial I} + \mathbf{K}\frac{\partial \boldsymbol{y}}{\partial I} + \boldsymbol{p}\frac{\partial F_{\mathrm{MR}}}{\partial I} = \mathbf{0}. \tag{12}$$

Notice that the kinematic excitation w does not depend on the current I therefore $\partial w/\partial I = 0$. The damper force sensitivity $\partial F_{\mathrm{MR}}/\partial I$ with respect to the control current is unknown yet. It is obtained by differentiating (3), (1c), (1d) with respect to I:

$$\frac{\partial F}{\partial I} = B_1 + \frac{\partial B_1}{\partial I}I + \frac{\partial D_1}{\partial I}, \tag{13a}$$

$$\frac{\partial \dot{s}}{\partial I} = -\frac{\partial f}{\partial I}s - f\frac{\partial s}{\partial I} + h_1\frac{\partial F}{\partial I}, \tag{13b}$$

$$\frac{\partial F_{\mathrm{MR}}}{\partial I} = \frac{\partial f}{\partial I} s + f \frac{\partial s}{\partial I} + h_2 \frac{\partial F}{\partial I}. \tag{13c}$$

The differential equations (1c) and (13b) are numerically integrated along with equations (11) and (12) during simulation. Both (11) and (12) sets of equations can be rewritten to one set of equations as follows:

$$\begin{aligned} \begin{bmatrix} \mathbf{M} & \mathbf{0} \\ \mathbf{0} & \mathbf{M} \end{bmatrix} \begin{bmatrix} \ddot{\boldsymbol{y}} \\ \dfrac{\partial \ddot{\boldsymbol{y}}}{\partial I} \end{bmatrix} + \begin{bmatrix} \mathbf{K} & \mathbf{0} \\ \mathbf{0} & \mathbf{K} \end{bmatrix} \begin{bmatrix} \boldsymbol{y} \\ \dfrac{\partial \boldsymbol{y}}{\partial I} \end{bmatrix} \\ + \begin{bmatrix} \mathbf{0} \\ \boldsymbol{p} \end{bmatrix} \frac{\partial F_{\mathrm{MR}}}{\partial I} + \begin{bmatrix} \boldsymbol{p} \\ \mathbf{0} \end{bmatrix} F_{\mathrm{MR}} = \begin{bmatrix} \boldsymbol{m} \\ \mathbf{0} \end{bmatrix} w, \end{aligned} \tag{14}$$

rewritten as

$$\mathbf{M}_{\mathrm{c}} \ddot{\boldsymbol{q}} + \mathbf{K}_{\mathrm{c}} \boldsymbol{q} + \boldsymbol{p}_1 \frac{\partial F_{\mathrm{MR}}}{\partial I} + \boldsymbol{p}_2 F_{\mathrm{MR}} = \boldsymbol{m}_{\mathrm{c}} w. \tag{15}$$

Equations (13) are second-order ordinary differential equations (ODE). Numerically it is beneficial to decrease second-order ODEs to first order as follows

$$\begin{aligned} \begin{bmatrix} \dot{\boldsymbol{q}} \\ \ddot{\boldsymbol{q}} \\ \dot{s} \\ \dfrac{\partial \dot{s}}{\partial I} \end{bmatrix}_{10\times 1} &= \begin{bmatrix} \mathbf{0} & \mathbf{I} & \mathbf{0} & 0 \\ -\mathbf{M}_{\mathrm{c}}^{-1}\mathbf{K} & \mathbf{0} & \mathbf{0} & 0 \\ \mathbf{0} & \mathbf{0} & -f & 0 \\ \mathbf{0} & \mathbf{0} & \dfrac{\partial f}{\partial I} & -f \end{bmatrix} \begin{bmatrix} \boldsymbol{q} \\ \dot{\boldsymbol{q}} \\ s \\ \dfrac{\partial s}{\partial I} \end{bmatrix} \\ &+ \begin{bmatrix} \mathbf{0} \\ -\mathbf{M}_{\mathrm{c}}^{-1}\boldsymbol{p}_1 \\ 0 \\ 0 \end{bmatrix} \frac{\partial F_{\mathrm{MR}}}{\partial I} + \begin{bmatrix} \mathbf{0} \\ -\mathbf{M}_{\mathrm{c}}^{-1}\boldsymbol{p}_2 \\ 0 \\ 0 \end{bmatrix} F_{\mathrm{MR}} \\ &+ \begin{bmatrix} \mathbf{0} \\ \mathbf{0} \\ h_1 \\ 0 \end{bmatrix} F + \begin{bmatrix} \mathbf{0} \\ \mathbf{0} \\ 0 \\ h_1 \end{bmatrix} \frac{\partial F}{\partial I} + \begin{bmatrix} \mathbf{0} \\ \mathbf{M}_{\mathrm{c}}^{-1}\boldsymbol{m}_{\mathrm{c}} \\ 0 \\ 0 \end{bmatrix} w \end{aligned} \tag{16}$$

rewritten as

$$\dot{\mathbf{X}} = \mathbf{A}\mathbf{X} + \mathbf{B}\frac{\partial F_{\mathrm{MR}}}{\partial I} + \mathbf{C}F_{\mathrm{MR}} + \mathbf{E}F + \mathbf{F}\frac{\partial F}{\partial I} + \mathbf{D}w. \tag{17}$$

This is the set of the ten first order ODEs. The first eight ODEs describe dynamics of the quarter car model (Fig. 3). The set of ODEs above can be moreover expanded by two extra ODEs (1c) and (13b) which are employed in the adaptive control

algorithm. Subsequently, $\partial F_{\mathrm{MR}}/\partial I$, $\partial F/\partial I$, F_{MR}, F values are evaluated from terms (13c), (13a), (1d) and (3) in each integration step.

The performance index in this study has been chosen in terms of minimizing sprung mass acceleration to ensure the best possible comfort:

$$J(t) = \ddot{y}_1(t)^2. \tag{18}$$

As the expression (18) shows, the performance index is not formulated as an integral criterion such that the adaptive control algorithm tries to minimize actual acceleration in each time step. According to (8), the sensitivity of the performance index with respect to the control current I is calculated from

$$\frac{\partial J}{\partial I} = 2\ddot{y}_1 \frac{\partial \ddot{y}_1}{\partial I}. \tag{19}$$

Finally, control current I for the next time step is evaluated from (7).

5. Simulation

The simulation of the 1/4 car model is implemented in the program MATLAB. The sine sweep excitation with decreasing amplitude is used for simulation study, as presented in Fig. 4. The sweeping frequency ranges from 0.5 to 4 Hz. The first

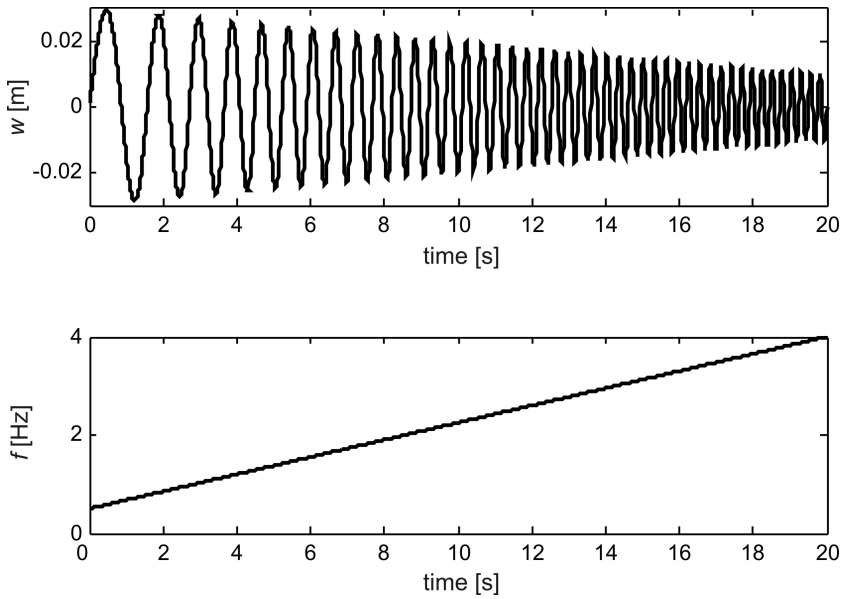

Fig. 4. Sine sweep excitation.

system resonant frequency is 1.2 Hz. The amplitude of signal linearly decreases with time from start (3 cm) to finish (1 cm). This excitation has been used to tune both control policies as well as to find optimal passive damping in the sense of minimizing acceleration dispersion (20) over the 20 second time interval:

$$D_{\ddot{y}_1} = E(\ddot{y}_1 - m_{\ddot{y}_1})^2. \tag{20}$$

Values of all system parameters are shown in Table 1, optimal skyhook gain S, adaptive algorithm gain μ, optimal current for passive suspension I_p can be found in Table 2.

Random high frequency excitation is considered (Fig. 5) to study performance of both controllers and passive system under different types of excitation, when the parameters are not optimally tuned. It is a random process with a narrow

T a b l e 1. Values of used parameters

MR damper model parameters		Suspension model parameters
$c_0 = 156$	$c_1 = 332$	$m_1 = 221$ kg
$k_0 = 3.97$	$k_1 = -1$	$m_2 = 31$ kg
$\alpha_0 = 45.86$	$\alpha_1 = 939.73$	$k_\mathrm{s} = 14230\ \mathrm{N \cdot m^{-1}}$
$\alpha_2 = -264$		$k_\mathrm{t} = 122500\ \mathrm{N \cdot m^{-1}}$
$h_0 = 0$	$h_1 = 0$	
$h_2 = 0$	$h_3 = 1$	
$\beta = 27$	$f = 200$	

T a b l e 2. Dispersion of car body acceleration resulting from the simulation

	Sine sweep excitation	Random excitation
	dispersion $D_{\ddot{y}_1}$ $[\mathrm{m^2 \cdot s^{-4}}]$	
Adaptive control ($\mu = 8 \cdot 10^{-4}$)	$3.0601 \cdot 10^3$	$0.8260 \cdot 10^3$
Skyhook control ($S = 55$)	$3.0387 \cdot 10^3$	$1.6722 \cdot 10^3$
Passive ($I_\mathrm{p} = 0 \cdot 19$ A)	$5.4917 \cdot 10^3$	$2.3663 \cdot 10^3$

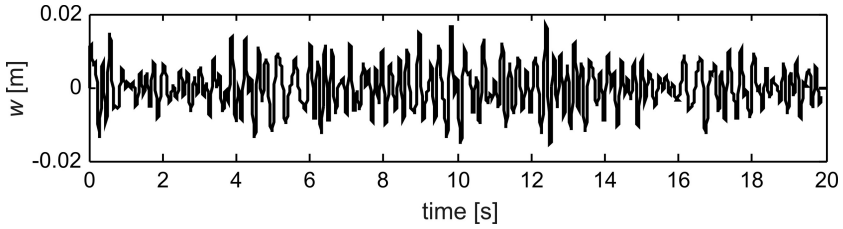

Fig. 5. Random high frequency excitation.

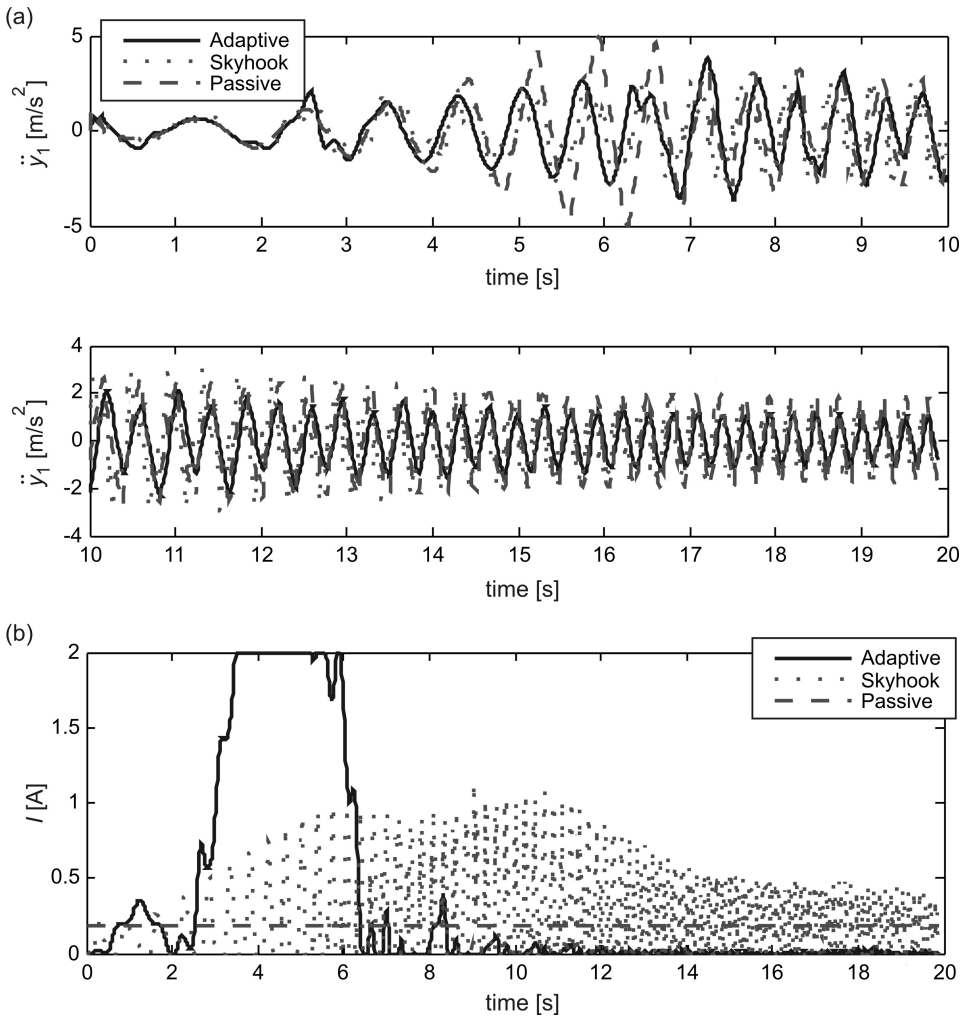

Fig. 6. a) car body acceleration with different control strategy, b) current to MR damper with different control strategy.

white noise PSD in the frequency range 2–6 Hz. Behaviour of the system along second resonant frequency 10.6 Hz related to un-sprung mass (tire and axles) is not considered in this simulation study.

Response of the system to the swept sine excitation over the 20 second interval is shown in Fig. 6a. According to the acceleration dispersion (Table 2) optimally tuned skyhook control shows slightly better performance than adaptive control and both controllers show considerably better performance than optimally tuned passive suspension. Moreover, according to Fig. 6a, skyhook control shows higher

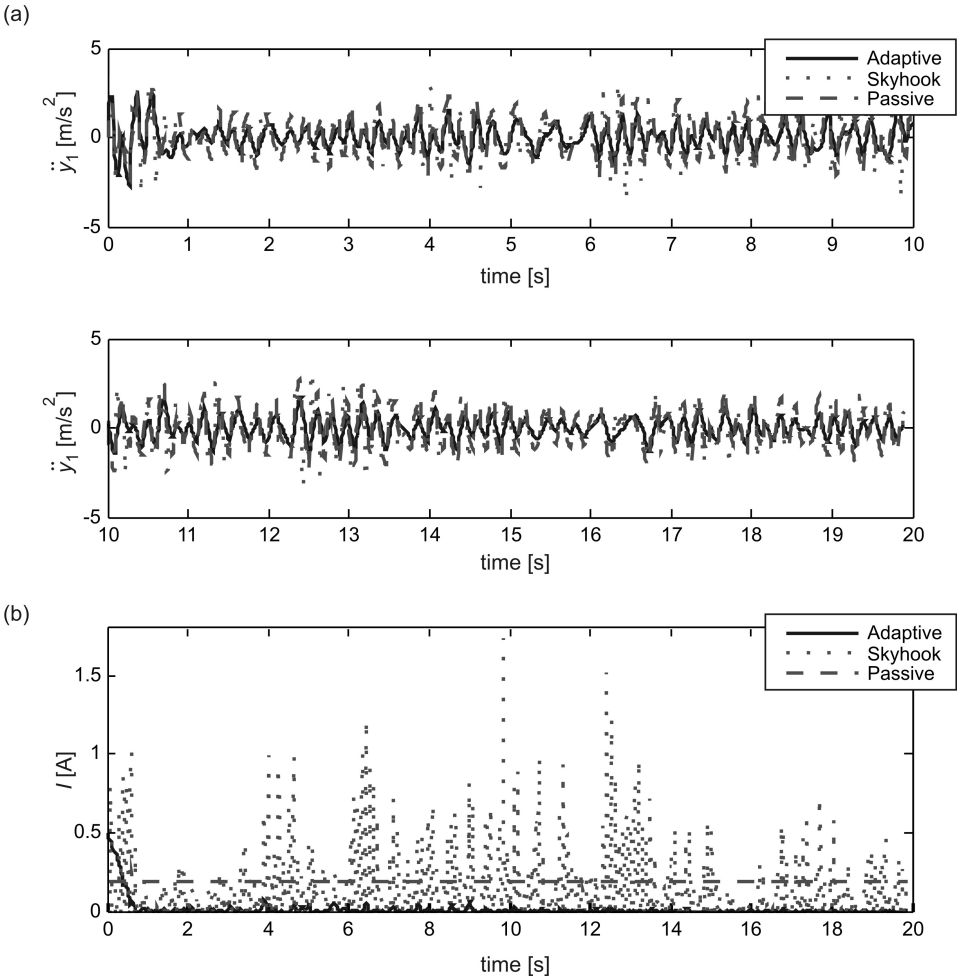

Fig. 7. a) car body acceleration with different control strategy, b) current to MR damper with different control strategy.

harmonics which result from sudden changes in the control current as shown in Fig. 6b. Adaptive control causes much smoother changes in current. While excitation frequency increases toward system resonant frequency, control current increases. Vice-versa the control current decreases behind the resonant frequency in order to minimize body acceleration.

A different situation occurs when the system is subjected to any other type of excitation represented by high frequency excitation (Fig. 5). Since the skyhook control and the passive suspension are not optimally tuned to such an excitation type, they show much worse performance in comparison to adaptive control

(Fig. 7a, Table 2). The skyhook gain S and also the passive current I_{p} should have been set lower in this case. Adaptive algorithm, which responds to excitation and system changes in real time, decreases control current from starting 0.5 A to approximately 0 A (Fig. 7b). This means minimum possible damping is required to minimize body acceleration in case of high frequency excitation.

6. Conclusion

Three different types of car suspension configuration have been studied in this paper. A new hysteretic MR damper model has been formulated from the existing parametric model. This model is able to describe nonlinear hysteretic behaviour of the real MR damper in the low frequency range where its parameters are identified. The size of the hysteretic loop in real MR damper changes with excitation frequency in a different way than in the MR damper model. Therefore the mentioned MR damper model shouldn't be used for wide frequency range simulations. This shortage can be removed by a more precise selection of the filter which describes hysteretic behaviour of MR damper. On the other hand, the simplicity of the proposed MR damper model allows easy derivation of the performance index sensitivity to the control current, which is necessary in the adaptive control algorithm.

Skyhook suspension, passive suspension and adaptive suspension have been compared to each other under two different types of excitation. All systems have been optimally tuned using sine sweep excitation for the purpose of minimizing body acceleration dispersion over a 20 s time interval. In this simulation skyhook suspension shows slightly better results than adaptive suspension, but higher harmonics occur in the body acceleration response. Passive suspension shows worse performance. Random excitation with high frequency range is used for the performance comparison of all the three suspension control systems, for excitation where their parameters are not optimally tuned. The adaptive control clearly shows the best performance due to its ability to react to system and excitation changes in real time. To ensure the better overall performance of the basic skyhook strategy, it can be augmented by extended ground-hook, which reduces tire deformations. Also a nonlinear extended sky-hook/ground-hook [12], which incorporates state dependent control gains, can improve the suspension performance over the different excitation types.

Moreover, it should be considered that the stability of the adaptive algorithm is not guaranteed in general. Convergence of the algorithm to the optimal control depends on the adaptive algorithm gain. Global stability can be reached by introducing Lyapunov stability criterion and choose the adaptive control law in such a way that the requirements of the stability criterion are fulfilled. That is why the global stability of the proposed algorithm should be investigated in the future.

Acknowledgements

This work was supported by the project VEGA No. 1/4093/07.

REFERENCES

[1] CROSBY, M. J.—KARNOP, D. C.: The Active Damper. The Shock and Vibration Bulletin 43, Washington, DC, Naval Research Laboratory 1973.
[2] AHMEDIAN, M.—REICHERT, B. A.: Shock and Vibration, *8*, 2001, p. 95.
[3] SONG, X. M.: Design of adaptive vibration control system with application to magnetorheological dampers. [Doctor of Philosophy Dissertation]. Blacksburg, Virginia, Virginia Polytechnic Institute and State University 1999.
[4] SONG, X.: Journal of Intelligent Materials and Structures, *16*, 2005, p. 421.
[5] STANWAY, R.—SPROSTON, J. L.: Journal of Electrostatics, *20*, 1987, p. 167.
[6] KWOK, N. M.—HA, Q. P.: Sensors and Actuators A, Physical, *132*, 2006, p. 441.
[7] WU, W. J.—CAI, C. S.: Journal of Vibration and Control, *12*, 2006, p. 67.
[8] NGUYEN, T. H.—KWOK, N. M.—HA, Q. P.—LI, J.—SAMALI, B.: Adaptive sliding mode control for civil structures using megnetorheological dampers. Tokyo, Japan, ISARC, Japan Robot Association 2006, p. 636.
[9] SONG, X.—AHMEDIAN, M.: Study of Semiactive Adaptive Control Algorithms with Magneto-Rheological Seat Suspension. SAE International 2004-01-1648, Warrendale, PA, 2004, p. 117.
[10] STEIN, G. J.—BALLO, I.: Vehicle System Dynamics, *20*, 1991, p. 57.
[11] MÚČKA, P.: Strojn. Cas., *51*, 2000, p. 174.
[12] VALÁŠEK, M.—KORTÜM, W.—ŠIKA, Z.—MADOLEN, L.—VACULÍN, O.: Control Engineering Practice, *6*, 1998, p. 735.
[13] SPENCER, B. F.—DYKE, S. J.—SAIN, M. K.—CARLSON, J. D.: ASCE Journal of Engineering Mechanics, *123*, 1997, p. 230.
[14] BARTKO, R.: In: Dynamics of Machines 2004: National colloquium with international participation. Praha, Ústav termomechaniky AV ČR 2004.
[15] BARTKO, R.: Machine Dynamics Problems, *30*, 2006, p. 30.

Received: 30.11.2007
Revised: 22.5.2008